

Theory of two-particle excitations and the magnetic susceptibility in high- T_c cuprate superconductors

S. BREHM¹, E. ARRIGONI², M. AICHHORN³, AND W. HANKE¹

¹ *Institute for Theoretical Physics and Astrophysics, University of Würzburg, Am Hubland, 97074 Würzburg, Germany*

² *Institute for Theoretical Physics and Computational Physics, Graz University of Technology, Petersgasse 16, 8010 Graz, Austria*

³ *Centre de Physique Théorique, École Polytechnique, 91128 Palaiseau Cedex, France*

PACS 74.72.Gh – Superconducting materials, cuprates, Hole doped compounds

PACS 74.25.Ha – Magnetic properties of superconductors

PACS 71.45.Gm – Correlations, collective effects

PACS 71.10.Fd – Hubbard model, electronic structure

PACS 74.25.Dw – Phase diagrams, superconductivity

Abstract. - Two-particle (2-p) excitations such as spin and charge excitations play a key role in high- T_c cuprate superconductors (HTSC). On the basis of a parameter-free theory, which extends the Variational Cluster Approach (a recently developed embedded cluster method) to 2-p excitations, the magnetic excitations of HTSC are shown to be reproduced for a Hubbard model within the relevant strong-coupling regime. In particular, the resonance mode in the underdoped regime, its intensity and “hour-glass” dispersion are in good overall agreement with experiments.

Introduction. – Two-particle (2-p) excitations and their corresponding magnetic, charge, optical and pairing susceptibilities are fundamental for obtaining a microscopic understanding of the high- T_c cuprate superconductor (HTSC) physics, complementing single-particle (such as angle-resolved photoemission (ARPES), etc.) experiments. A key example is provided by the magnetic excitations: When entering the superconducting (SC) state in the high- T_c cuprates, the magnetic excitation spectrum is characteristically and markedly modified: a resonant mode emerges with its peak intensity being highest around the wave vector $\mathbf{q}_{AF} = (\pi, \pi)$ characteristic of antiferromagnetism (AF) in the undoped parent compound [1, 6]. Its frequency $\omega_{\text{res}}(\mathbf{q}_{AF})$ follows the doping dependence of T_c . Away from \mathbf{q}_{AF} , the mode has both a downward and upward “hour-glass”-like dispersion. A variety of experiments in the HTSC, such as photoemission, optical and tunneling spectroscopies, have been interpreted as evidence of interactions of electrons with this mode [7]. However its microscopic origin, in particular its role in pairing and the more detailed effects arising from the interactions of charge carriers with this magnetic mode are still unclear and intensively debated [11]. A prerequisite to resolve this debate obviously requires a consistent theoretical description of the neutron resonance mode and,

more generally, the magnetic excitation spectrum [18] and at the same time of the phase diagram, containing the competing AF and SC phases.

In this letter, on the basis of a microscopic theory for 2-p excitations, we provide such a consistent description for the experimentally relevant regime of the two-dimensional (2D) Hubbard model. The essential new points here are that our theory for 2-p excitations (e.g. the dynamic spin-susceptibility) is (i) parameter-free (given fixed, widely-accepted values for the Hubbard model parameters) and (ii) is working in the relevant strong correlation regime of the underlying Hubbard model. Previous descriptions of the magnetic resonance have been obtained by weak-coupling [21] and/or semiphenomenological approaches [23, 28] reproducing the experimental behavior with adjustable parameters. An accurate description of the infinite lattice is crucial in order to obtain the magnetic resonance which may be considered as a “fingerprint” of the AF order in the SC state. Only then are we able to differentiate between the competing AF and SC orders in the phase diagram. Therefore, the infinite-lattice limit (not to be confused with the limit of infinite dimensions) has also to be embedded in a controlled description of the corresponding susceptibilities.

We extend the original idea of the Variational Cluster

Approach (VCA), which is to extrapolate cluster results to the infinite lattice, to the treatment of 2-p excitations. In our novel approach, the 2-p vertex extracted from the corresponding cluster susceptibilities is used to obtain the susceptibilities for an infinite lattice. The VCA was recently applied to calculate the zero-temperature ($T=0$) phase diagram as well as single-particle excitations [30, 32, 33] of the single-band Hubbard model. These results successfully reproduced salient experimental features such as the electron-hole asymmetry in the doping dependence of AF and SC phases [32, 33] in the HTSC materials. Also the VCA single-particle excitations were found to reproduce characteristic features observed in ARPES experiments. In particular, in Ref. [37], the magnitude and doping dependence of the SC gap near the nodal and antinodal regions was studied in detail, and shown to reproduce qualitatively the much-discussed presence of a gap dichotomy of the nodal and antinodal SC gaps. Combined with the new results for 2-p magnetic excitations, presented in this work, a consistent picture emerges, which lends substantial support to Hubbard-model descriptions of high- T_c cuprate superconductivity.

For the appropriate strongly correlated regime ($U = 8t$) of the underdoped Hubbard model the resonance is obtained in a parameter-free calculation and verified to be a spin $S = 1$ excitonic bound state, which appears in the SC-induced gap in the spectrum of electron-hole spin-flip (i.e. $S = 1$) excitations. This will be detailed in our results, where we find the doping dependence of $\omega_{\text{res}}(\mathbf{q}_{AF})$, the energy-integrated spectral weight evaluated at \mathbf{q}_{AF} and the difference of the magnetic susceptibilities in the SC and the normal (N) states to be in qualitative accord with neutron scattering data for underdoped $\text{YBa}_2\text{Cu}_3\text{O}_{6+x}$ (YBCO), where the mode was studied in great detail [1, 6]. A spin excitonic bound state has previously been suggested on the basis of an itinerant picture, most frequently invoking a weakly correlated RPA-like form of the dynamic spin susceptibility (for a recent reference see, for example, Ref. [21]). As a weak-coupling form it leads to a Fermi-liquid like $\chi(q, \omega)$, which is in contrast to some of the anomalous dynamics found in neutron scattering experiments [1, 6]. On the other hand, when the 2-p interaction and the SC gap are used as adjustable parameters, it qualitatively accounts for the mode behavior near optimal and overdoped regimes [21].

Model and Method. – We start from the two-dimensional Hubbard model:

$$H = - \sum_{ij\sigma} t_{ij} c_{i\sigma}^\dagger c_{j\sigma} + U \sum_i n_{i\uparrow} n_{i\downarrow}, \quad (1)$$

where t_{ij} denote nearest (t) neighbor and next-nearest ($t' = -0.3t$) neighbor hopping matrix elements, $c_{i\sigma}^\dagger$ and $c_{j\sigma}$ are the usual creation and destruction operators, $n_{i\sigma}$ their density and $U = 8t$ the local Hubbard repulsion.

We consider the following matrix expression for the

transverse spin susceptibility:

$$\chi(\mathbf{Q}, i\omega_m^b) = \chi^0(\mathbf{Q}, i\omega_m^b) + \chi^0(\mathbf{Q}, i\omega_m^b) \mathbf{\Gamma}(\mathbf{Q}, i\omega_m^b) \chi(\mathbf{Q}, i\omega_m^b), \quad (2)$$

with the bosonic Matsubara frequencies $\omega_m^b = 2m\pi T$ and T the temperature.

Within our embedded cluster approach, the susceptibility χ depends on the wave vector \mathbf{Q} in the reduced Brillouin zone (BZ) associated with the superlattice produced by the clusters. In addition, χ is considered as a matrix in the cluster-site indices i and j and the products in Eq. (2) are matrix products. Its definition is given by

$$\chi_{ij}(\mathbf{Q}, i\omega_m^b) \equiv \int_0^\beta d\tau e^{i\omega_m^b \tau} \langle S_i^-(\mathbf{Q}, \tau) S_j^+(-\mathbf{Q}, 0) \rangle, \quad (3)$$

with the mixed representation for the spin operator

$$S_i^a(\mathbf{Q}, \tau) = \frac{1}{N_{cl}} \sum_{\mathbf{R}} S_{i+\mathbf{R}}^a(\tau) e^{i\mathbf{Q}\cdot\mathbf{R}}. \quad (4)$$

Here, the sum is carried out over all clusters, whose position is given by the vector \mathbf{R} , N_{cl} is the number of clusters, $S_{i+\mathbf{R}}^a$ is the a component of the spin operator at site $i + \mathbf{R}$ and τ is the usual imaginary time.

In Eq. (2), an effective particle-hole interaction (matrix) $\mathbf{\Gamma}$ is introduced, obtained from an average of the 2-p vertex over the additional internal frequencies and momenta¹ Eqs.(2-4) as well as the following discourse can straightforwardly be generalized to other 2-p susceptibilities, such as the charge response function, by replacing the spin operator in Eq. (3) by the corresponding charge density operator.

The “bubble” susceptibility χ^0 in (2) is obtained as a convolution of the “dressed” VCA one-particle (1-p) Green’s functions, i.e.

$$\chi_{ij}^0(\mathbf{Q}, i\omega_m^b) = -\frac{T}{N_{cl}} \sum_{n, \mathbf{K}} \left(G_{ij\uparrow}^{VCA}(\mathbf{K} + \mathbf{Q}, i\omega_n^f + i\omega_m^b) G_{ji\downarrow}^{VCA}(\mathbf{K}, i\omega_n^f) + F_{ij}^{VCA}(\mathbf{Q} - \mathbf{K}, i\omega_m^b - i\omega_n^f) F_{ji}^{*VCA}(\mathbf{K}, i\omega_n^f) \right). \quad (5)$$

¹ Notice that, besides this approximation, Eq. (2) is the well-known Bethe-Salpeter equation, which is in principle exact and valid for arbitrary interaction and is not limited to weak coupling as the RPA approximation. Neglecting the explicit dependence of the internal momenta and frequencies has been found to be a reasonable approximation in finite- T single-cluster QMC calculations [38] and in an extension of the Dynamical Cluster Approximation (DCA) to 2-p susceptibility calculations [39]. However, we would like to stress that, while the Eq. (2) appears formally similar to the equation used in Ref. [39] for DCA 2-p quantities, subtle differences occur in building up the self-consistent (spin-) response within a cluster: This is due to the fact that in the DCA (in contrast to our present VCA-type scheme) each cluster site “sees” the same mean-field. We have found, as shown e.g. in the “consistency number” α (Eq. (6,7)), the present scheme to give significantly improved results for comparable cluster sizes.

Here, $i\omega_n^f = (2n + 1)\pi T$ denote fermionic Matsubara frequencies, G^{VCA} are normal and F^{VCA} anomalous (i. e. characteristic of the SC state) fully interacting Green's functions obtained within the VCA and expressed in a mixed representation analogous to (4), and \mathbf{K} is again a vector of the reduced BZ.

Within the VCA [30], the self-energy of a so-called “reference system” is used as an approximation to the one of the physical system. The reference system typically consists of a subcluster of the original system in which single-particle terms can be “optimized” to obtain a stationary point of the grand potential for the infinite lattice. In a similar spirit, the effective interaction Γ in Eq. (2) is obtained from the corresponding cluster quantity,

$$\Gamma(i\omega_m^b) = \alpha [(\chi_{\text{cluster}}^0(i\omega_m^b))^{-1} - (\chi_{\text{cluster}}(i\omega_m^b))^{-1}] \quad (6)$$

(cf. also Ref. [40]). Note, that this vertex is defined on the cluster and thus independent of \mathbf{Q} . In Eq. (6), χ_{cluster}^0 is calculated via the same convolution as in (5), but using the exact single-particle cluster Green's functions, and χ_{cluster} is the exact cluster susceptibility. The latter quantities are obtained via Lanczos exact diagonalization.

In Eq. (6), we have introduced a multiplicative constant α , which is *not* a free parameter, but rather it is fixed by enforcing the sum rule for the transverse spin susceptibility:

$$\frac{T}{N_{cl}} \sum_{\mathbf{Q}, i\omega_m^b} \chi_{ii}(\mathbf{Q}, i\omega_m^b) = \langle S_i^- S_i^+ \rangle \quad (7)$$

In our parameter-free approach, the value of α can be used to assess the quality of our 2-p scheme: when α is close to 1, the cluster vertex is a good approximation to the vertex of the infinite lattice (see Fig. 1b). The quality of this approximation obviously depends on the cluster size L_c , and is expected to become exact for $L_c \rightarrow \infty$, where also $\alpha \rightarrow 1$. It also certainly depends on the ratio $\frac{t}{U}$ and on doping. We expect the method to give better results at strong coupling, where short-range effects dominate and are, thus, well accounted for by modest cluster sizes. Below, we provide some results in support of this expectation. After Fourier transforming over the cluster sites, the spin susceptibility $\chi(\mathbf{Q} + \mathbf{k}, \mathbf{Q} + \mathbf{k}', i\omega_m^b)$ acquires a dependence on two momenta due to the translation symmetry breaking introduced by the cluster tiling. The *physical* translation-invariant susceptibility $\chi(\mathbf{q}, i\omega_m^b)$, with $\mathbf{q} = \mathbf{Q} + \mathbf{k}$ is taken to be its diagonal part $\chi(\mathbf{Q} + \mathbf{k}, \mathbf{Q} + \mathbf{k}, i\omega_m^b)$.

Results. – Fig. 1a displays our results for the $\mathbf{q} = \mathbf{q}_{AF}$ part of the transverse spin spectral function $\text{Im}\chi^\pm(\mathbf{q} = \mathbf{q}_{AF}, \omega)$ at half-filling, i.e. in the AF phase, for different cluster sizes $L_c = 2 \times 2$, 4×2 and $\sqrt{10} \times \sqrt{10}$. Here, a “finite-size” gap appears, which continuously diminishes with increasing cluster sizes (Fig. 1a). It is comforting to note that the controlling constant α is very close to and also continuously decreasing towards $\alpha = 1$ as a function of increasing cluster size (Fig. 1b).

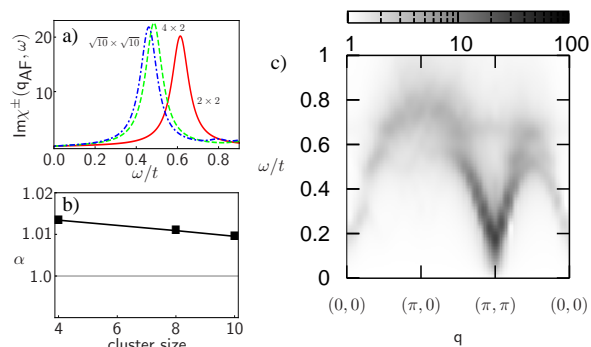


Fig. 1: VCA calculation for the 2D Hubbard model ($U = 8t$): (a) The imaginary part of the susceptibility $\chi^\pm(\mathbf{q}_{AF}, \omega)$ at half filling and (b) the sum-rule constant α as a function of the cluster size at half-filling; (c) $\text{Im}\chi^\pm(\mathbf{q}, \omega)$ intensity plot at 4% hole doping.

Fig. 1c shows the corresponding intensity plot for $\text{Im}\chi^\pm(\mathbf{q}, \omega)$ with remnants of the spin-density wave dispersion for a $L_c = 2 \times 4$ “reference” cluster at 4% hole doping. Results obtained with different cluster sizes reveal that at finite doping “finite-size” effects are of minor importance compared to the half-filled situation. We attribute this to a screening effect, which renders the 2-p vertex Γ significantly more short-ranged, i.e. more local. This means that it can accurately be extracted from the exact diagonalization of relatively small clusters.

Our results for the magnetic response properties in the SC state are shown in Fig. 2. Fig. 2a displays a density plot of the spin spectral function at $x=0.18$ doping (3×3 “reference” cluster). The magnetic resonance emerges in the SC-induced gap of $S = 1$ electron-hole (e-h) excitations when entering this SC doping regime. In Fig. 2a, we plot the intensity in the (ω, \mathbf{q}) -plane along the diagonal of the 2D-BZ. The celebrated “hour-glass” structure observed in the experiments (see, in particular, Ref. [6]) is very well reproduced in our calculation. The structure has its maximum spectral weight confined to a region close to \mathbf{q}_{AF} and a dramatic intensity reduction around $\simeq 0.8(\pi, \pi)$.

Our results confirm the experimental interpretation put forward in Ref. [6]. As shown in a density plot in Fig. 2b, we find for the same doping as in Fig. 2a ($x = 0.18$) a typical Fermi surface closed around (π, π) . Fig. 2c plots the corresponding e-h continuum (i.e. $S = 1$, spin-flip e-h excitations), obtained in our VCA calculation. Only collective modes below the e-h continuum (red line) can actually be detected, because modes within the continuum are Landau damped. This e-h continuum corresponds to Fig. 4c in Ref. [6]. The continuum threshold exhibits also in our case a pronounced minimum in the vicinity of the wave vector $2\mathbf{k}_N \simeq 0.8(\pi, \pi)$, which corresponds to scattering between nodes of the d-wave gap function (Fig. 2b gives just one quadrant of the BZ). The minimum in our

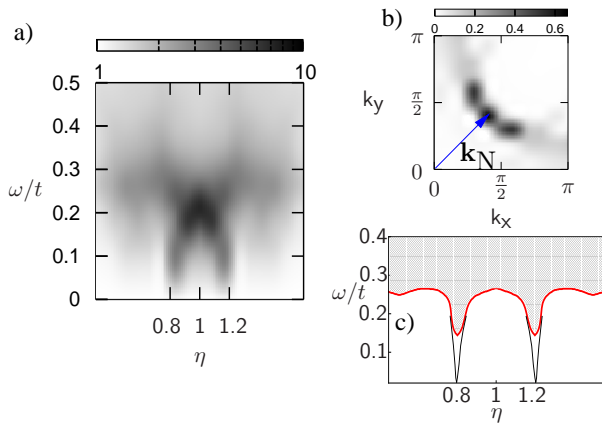


Fig. 2: (a) Intensity plot of $\text{Im}\chi^\pm(\mathbf{q}, \omega)$ from the microscopic 2-p theory Eqs. (2-7) along $\mathbf{q} = \eta(\pi, \pi)$ displaying the “hour-glass” shape. (b) Intensity plot of the low-energy spectral weight obtained from the corresponding VCA calculation for the 1-p spectral weight displaying the Fermi surface with the nodal scattering vector $2\mathbf{k}_N \simeq 0.8(\pi, \pi)$. (c) Spin-flip electron-hole continuum (hatched area: extracted from Eq. (3)) with a minimum at $2\mathbf{k}_N$. All results are obtained in the SC phase at $x = 0.18$.

calculation is, however, not so steep as in the idealistic situation in Fig. 4c of Ref. [6], due to correlation effects and to a broadening of $0.05t$ used for the exact diagonalization.

We would like to emphasize that a similar picture has been suggested in RPA-like descriptions of the neutron resonance (see, for example, Ref. [21]). However, in these calculations the d-wave gap amplitude as well as the magnitude of the effective 2-p interaction have been introduced as adjustable parameters in order to reproduce the experimental energy positions of the resonance mode at (π, π) and the e-h threshold around $0.8(\pi, \pi)$.

In Figs. 3a to 3c, we show additional comparisons of our calculations with salient features of the neutron scattering experiments in underdoped $\text{YBa}_2\text{Cu}_3\text{O}_{6+x}$ [41]: Fig. 3a displays the difference ($\text{Im}\Delta\chi^\pm(\mathbf{q}_{AF}, \omega)$) between the spin spectral functions in the SC and in the N phases. The neutron results by Fong et al. [41] (left panel) are compared with our results (right panel). Since we are using a $T = 0$ method, our “normal-state” solutions have been obtained by forcing the SC Weiss field to be zero in the variational procedure. Furthermore, the dopings in the experimental and in the theoretical curves do not exactly coincide, although both are in the underdoped region. In this sense, our comparison is only qualitative. Nevertheless, our calculations reproduce the experimental finding, that the enhancement of the spectral weight around the resonance peak energy is accompanied by a reduction of the spectral weight over a limited energy range both above and below $\omega_{\text{res}}(\mathbf{q}_{AF})$.

Fig. 3b compares the energy-integrated spin spectral weight at \mathbf{q}_{AF} obtained in experiment at various dopings [41] (left panel) with our theoretical results (right)

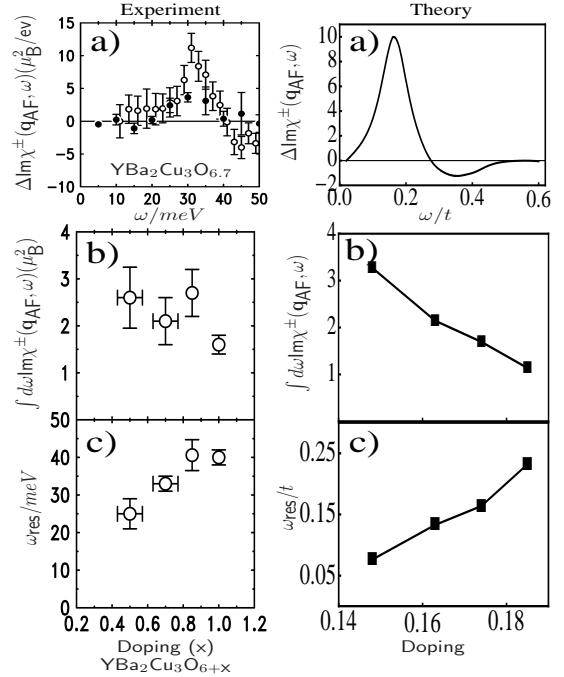


Fig. 3: Comparisons of our theoretical results with experiment (reprinted with kind permission from Ref. [41] “Copyright (2000) by the American Physical Society”): (a) Difference between $\text{Im}\chi(\mathbf{q}_{AF}, \omega)$ in the SC and normal states (theory: $x = 0.17$); (b) ω -integrated spectral weight at \mathbf{q}_{AF} ; (c) ω_{res} as a function of doping.

in the SC region. The overall doping dependence is similar. Finally, in Fig. 3c, the doping behavior of the energy of the magnetic resonance is compared in the underdoped regime ($x = 1$ corresponds in experiment to optimal doping). Again a similar trend is observed.

Summary and conclusions. – In summary, our novel theory for 2-p excitations is able to provide an appropriate description of the resonance mode in HTSC in good agreement with experiments. In particular, the calculated doping dependence of $\omega_{\text{res}}(\mathbf{q}_{AF})$, the “hour-glass” dispersion of the resonance and its rapid decrease around a characteristic wave vector $2\mathbf{k}_N$, which coincides with the distance between nodal points on the Fermi surface, are qualitatively consistent with the experiment and support the $S = 1$ magnetic exciton scenario. In contrast to previous calculations, our results are obtained in the appropriate strong-correlation regime and contain no adjustable parameters. When taken together with earlier results on the phase diagram and single-particle excitations, they constitute a rather strong support for a Hubbard-model description of the HTSC materials.

It is a pleasure to thank M. Pothhoff, D.J. Scalapino and S. Hochkeppel for discussions. The work is supported by the Deutsche Forschungsgemeinschaft within

the Forschergruppe FOR 538 and by the Austrian Science Fund (FWF), grants P18551-N16 and J2760-N16.

REFERENCES

- [1] ROSSAT-MIGNOD J., REGNAULT L. P., VETTER C., BOURGES P., BURLET P., BOSSY J., HENRY J. Y. and LEPERTOT G., *Physica C*, **185–198** (1991) 86
- [2] ARAI M., NISHIJIMA T., ENDOH Y., EGAMI T., TAJIMA S., TOMIMOTO K., SHIOHARA Y., TAKAHASHI M., GARRETT A. and BENNINGTON S. M., *Phys. Rev. Lett.*, **83** (1999) 608
- [3] REZNIK D., BOURGES P., PINTSCHOVIVUS L., ENDOH Y., SIDIS Y., MASUI T. and TAJIMA S., *Phys. Rev. Lett.*, **93** (2004) 207003
- [4] SIDIS Y., PAILHÈS S., HINKOV V., FAUQUE B., ULRICH C., CAPOGNA L., IVANOV A., REGNAULT L.-P., KEIMER B. and BOURGES P., *C. R. Phys.*, **8** (2007) 745
- [5] HINKOV V., BOURGES P., PAILHÈS S., SIDIS Y., IVANOV A., FROST C. D., PERRING T. G., LIN C. T., CHEN D. P. and KEIMER B., *Nature Physics*, **3** (2007) 780
- [6] PAILHÈS S., SIDIS Y., BOURGES P., HINKOV V., IVANOV A., ULRICH C., REGNAULT L. P. and KEIMER B., *Phys. Rev. Lett.*, **93** (2004) 167001
- [7] See, for example
- [8] BORISENKO S. V., KORDYUK A. A., KIM T. K., KOITZSCH A., KNUPFER M., FINK J., GOLDEN M. S., ESCHRIG M., BERGER H. and FOLLATH R., *Phys. Rev. Lett.*, **90** (2003) 207001
- [9] HWANG J., TIMUSK1 T. and GU G. D., *Nature*, **427** (2004) 714
- [10] ZASADZINSKI J. F., OZYUZER L., MIYAKAWA N., GRAY K. E., HINKS D. G. and KENDZIORA C., *Phys. Rev. Lett.*, **87** (2001) 067005
- [11] See, for example
- [12] VOJTA M., VOJTA T. and KAUL R. K., *Phys. Rev. Lett.*, **97** (2006) 097001
- [13] UHRIG G. S., SCHMIDT K. P. and GRÜNINGER M., *Phys. Rev. Lett.*, **93** (2004) 267003
- [14] KEE H.-Y., KIVELSON S. A. and AEPPLI G., *Phys. Rev. Lett.*, **88** (2002) 257002
- [15] ABANOV A., CHUBUKOV A. V., ESCHRIG M., NORMAN M. R. and SCHMALIAN J., *Phys. Rev. Lett.*, **89** (2002) 177002
- [16] NORMAN M. R., *Phys. Rev. B*, **63** (2001) 092509
- [17] ESCHRIG M., *Adv. Phys.*, **55** (2006) 47
- [18] KASTNER M. A., BIRGENEAU R. J., SHIRANE G. and ENDOH Y., *Rev. Mod. Phys.*, **70** (1998) 897
- [19] KEIMER B., BIRGENEAU R. J., CASSANHO A., ENDOH Y., ERWIN R. W., KASTNER M. A. and SHIRANE G., *Phys. Rev. Lett.*, **67** (1991) 1930
- [20] KEIMER B., BELK N., BIRGENEAU R. J., CASSANHO A., CHEN C. Y., GREVEN M., KASTNER M. A., AHARONY A., ENDOH Y., ERWIN R. W. and SHIRANE G., *Phys. Rev. B*, **46** (1992) 14034
- [21] For a recent work see
- [22] EREMİN I., MORR D. K., CHUBUKOV A. V., BENNEMANN K. H. and NORMAN M. R., *Phys. Rev. Lett.*, **94** (2005) 147001
- [23] See, for example
- [24] ABANOV A. and CHUBUKOV A. V., *Phys. Rev. Lett.*, **83** (1999) 1652
- [25] SEGA I., PRELOVSEK P. and BONCA J., *Phys. Rev. B*, **68** (2003) 054524
- [26] PRELOVŠEK P. and SEGA I., *Phys. Rev. B*, **74** (2006) 214501
- [27] ZEYHER R., *Theory of the hourglass dispersion of magnetic excitations in high - t_c cuprates* arXiv:0810.4857 (2008)
- [28] DEMLER E. and ZHANG S.-C., *Phys. Rev. Lett.*, **75** (1995) 4126
- [29] DEMLER E., HANKE W. and ZHANG S.-C., *Rev. Mod. Phys.*, **76** (2004) 909
- [30] POTTHOFF M., AICHHORN M. and DAHNKEN C., *Phys. Rev. Lett.*, **91** (2003) 206402
- [31] DAHNKEN C., AICHHORN M., HANKE W., ARRIGONI E. and POTTHOFF M., *Phys. Rev. B*, **70** (2004) 245110
- [32] SÉNÉCHAL D., LAVERTU P. L., MAROIS M. A. and TREMBLAY A. M. S., *Phys. Rev. Lett.*, **94** (2005) 156404
- [33] AICHHORN M. and ARRIGONI E., *Europhys. Lett.*, **72** (2005) 117
- [34] AICHHORN M., ARRIGONI E., POTTHOFF M. and HANKE W., *Phys. Rev. B*, **74** (2006) 024508
- [35] AICHHORN M., ARRIGONI E., POTTHOFF M. and HANKE W., *Phys. Rev. B*, **76** (2007) 224509
- [36] AICHHORN M., ARRIGONI E., POTTHOFF M. and HANKE W., *Phys. Rev. B*, **74** (2006) 235117
- [37] AICHHORN M., ARRIGONI E., HUANG Z. B. and HANKE W., *Phys. Rev. Lett.*, **99** (2007) 257002
- [38] BULUT N., SCALAPINO D. J. and WHITE S. R., *Physica C*, **246** (1995) 85
- [39] HOCHKPEPPEL S., ASSAAD F. F. and HANKE W., *Phys. Rev. B*, **77** (2008) 205103
- [40] JARRELL M., MAIER T., HUSCROFT C. and MOUKOURI S., *Phys. Rev. B*, **64** (2001) 195130
- [41] FONG H. F., BOURGES P., SIDIS Y., REGNAULT L. P., BOSSY J., IVANOV A., MILIUS D. L., AKSAY I. A. and KEIMER B., *Phys. Rev. B*, **61** (2000) 14773.